

Comparison Between COMSOL Multiphysics[®] and STAR-CCM+[®] Simulation Results and Experimentally Determined Measured Data for a Venturi Tube

A. Diring, L. Fromme, M. Petry, E. Weizel*

Department of Engineering Sciences and Mathematics, Bielefeld University of Applied Sciences, Bielefeld, Germany

*Corresponding author: Interaktion 1, 33619 Bielefeld, Germany; ernst.weizel@fh-bielefeld.de

Abstract: Numerical simulation tools offer the opportunity to ascertain characteristic values for fluid flows, which are difficult to measure. This work describes the examination of a turbulent flow in a Venturi tube using two different commercial CFD tools, namely COMSOL Multiphysics[®] and STAR-CCM+[®]. The simulation models are validated by experimentally determined measured data.

Keywords: CFD, Venturi tube, turbulent flow, $k-\varepsilon$ turbulence model, $k-\omega$ turbulence model

1. Introduction

Nowadays, a common problem in engineering is to ascertain characteristic values of technical systems. Real measurements may not be performed due to high costs or the difficulty to measure without producing disturbances in a system. In such cases simulation tools can provide the desired results. COMSOL Multiphysics[®] is a suitable tool for modeling physics-based problems using the finite element method (FEM). STAR-CCM+[®] instead is based on the finite volume method (FVM). Both tools can be used for CFD problems in the laminar as well as in the turbulent regime. Different turbulence models are provided for different applications.

The Venturi effect is a well-known phenomenon in fluid mechanics. Many industries developing equipment and machines take advantage of the Venturi effect; for example, carburetors, atomizer, nebulizer, and sprayers. Automated pool cleaners use the Venturi effect to draw debris and sediment into collection tubes. Sand blasters also utilize the low-pressure area created by flowing air to suck sand into their systems and mix it with the flow.

Besides these applications the Venturi effect is also used in scientific laboratories and in

industrial applications for measuring the flow rate of fluids. Volume flows can be determined by using Bernoulli's equation and the differential pressure between the narrowest and the largest cross section (Fig. 1).

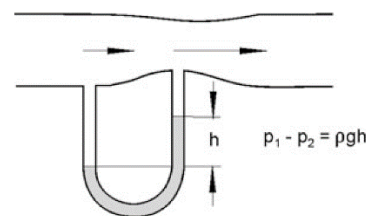


Figure 1. Measurement of a volume flow using a Venturi nozzle. [1]

2. Set-up

2.1 Experimental Set-up

A Venturi tube is built up in the Laboratory for Fluid Mechanics at the Bielefeld University of Applied Sciences. Pressure sensors are used to measure the pressure difference between the narrowest and the widest cross section of the tube for different flow velocities. This data is used to validate the CFD simulations. A characteristic curve for the system can be ascertained by the relation between the differential pressure and the flow velocity.

The experimental assembly consists of the union of 3 separate tubes with a total length of 4.4 m. The first part is a tube with an internal diameter of 0.1 m and a length of 2.0 m. The following part is the Venturi tube, which is 0.4 m long with an internal diameter of 0.05 m at the narrowest cross section in the middle of the tube. The third part is equivalent to the first one.

At one end of the tube a fan is mounted which can produce air flows with variable flow velocities. In the following figure 2 the complete test set-up is shown.



Figure 2. Experimental set-up in the Laboratory for Fluid Mechanics at the Bielefeld University of Applied Sciences

As figure 3 illustrates, differential pressures can be measured between seven different points at the outer contour of the Venturi tube. The difference between the low pressure in the middle of the tube (p-4) and the higher pressure at the inlet (p-1) and the outlet (p-7) are of special interest in this work. Between two neighbouring measuring points the distance equals 6.3 cm, respectively.



Figure 3. Venturi tube with connected pressure measuring pipes

2.2 Model Set-up

In both simulation tools a 2D axis symmetrical model is developed. The outside contour is built by applying a parametric curve utilizing a cosine function:

$$r(z) = 0.0125 \text{ m} \cos\left(\frac{2\pi}{0.32 \text{ m}} z\right) + 0.0375 \text{ m} \quad (1)$$

Figure 4 shows the contour of the Venturi tube in COMSOL Multiphysics®. The red line is the symmetry axis. Figure 5 displays the entire geometry of the Venturi model similar to the experimental set-up.

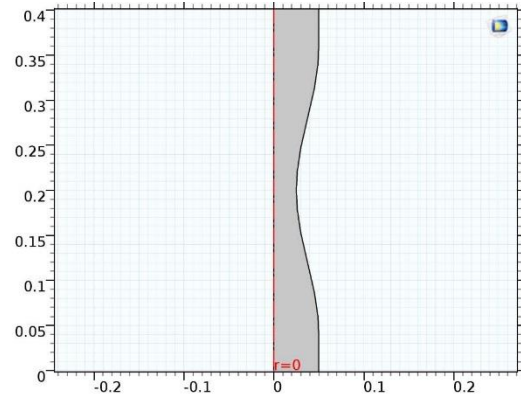


Figure 4. Contour of the Venturi tube

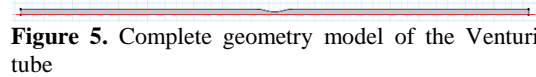


Figure 5. Complete geometry model of the Venturi tube

We use a fine mapped quadrilateral mesh with additional boundary layers in both simulation programs. A mesh study was performed, to find a suitable mesh for the used turbulence models in both tools. Finally, a quadrilateral mesh with 3000 elements in axial direction and 30 elements in radial direction with 10 additional boundary layers is used for the comparison between the numerical and experimental results.

In COMSOL Multiphysics® a finite element mesh and in STAR-CCM+® a finite volume mesh is used. Figure 6 displays the comparison between both discretisations of the fluid domain.

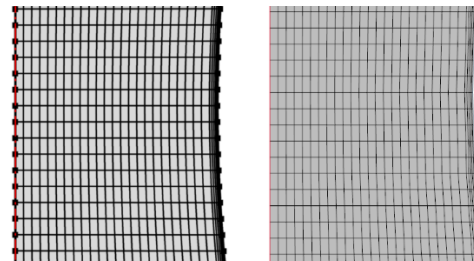


Figure 6. FE mesh in COMSOL Multiphysics® (left side) and FV mesh STAR CCM+® (right side)

3. Governing Equations

In this model, the turbulent air flow is assumed to be incompressible and isothermal. Furthermore, only stationary flow problems for various flow velocities are solved.

The continuity equation [2] simplifies to

$$\nabla \cdot \mathbf{u} = 0 \quad (2)$$

and the Navier-Stokes equations to

$$\rho(\mathbf{u} \cdot \nabla)\mathbf{u} = \nabla \cdot [-p\mathbf{I} + (\mu + \mu_T)(\nabla\mathbf{u} + (\nabla\mathbf{u})^T)] + \mathbf{F} \quad (3)$$

For the turbulent, single phase flow simulation the k - ε and the k - ω turbulence models are used. At first the equations for the k - ε model are described.

3.1 k - ε Turbulence Model

The time independent transport equation for the turbulent kinetic energy k is defined as follows:

$$\rho(\mathbf{u} \cdot \nabla)k = \nabla \cdot \left(\left(\mu + \frac{\mu_T}{\sigma_k} \right) \nabla k \right) + P_k - \rho\varepsilon \quad (4)$$

with the turbulent viscosity

$$\mu_T = \rho C_\mu \frac{k^2}{\varepsilon}$$

and the production term

$$P_k = \mu_T (\nabla\mathbf{u} : (\nabla\mathbf{u} + (\nabla\mathbf{u})^T)).$$

The time independent transport equation for the turbulent dissipation rate ε can be written as:

$$\rho(\mathbf{u} \cdot \nabla)\varepsilon = \nabla \cdot \left(\left(\mu + \frac{\mu_T}{\sigma_\varepsilon} \right) \nabla \varepsilon \right) + C_{\varepsilon 1} \frac{\varepsilon}{k} P_k - C_{\varepsilon 2} \rho \frac{\varepsilon^2}{k} \quad (5)$$

The k - ε model constants are predefined by default as [2]:

$$C_{\varepsilon 1} = 1.44; \quad C_{\varepsilon 2} = 1.92; \quad C_\mu = 0.09; \\ \sigma_k = 1; \quad \sigma_\varepsilon = 1.3$$

3.2 k - ω Turbulence Model

The equations for the k - ω turbulence model are quite similar to the k - ε model equations.

The time independent transport equation for the turbulent kinetic energy k reads:

$$\rho(\mathbf{u} \cdot \nabla)k = \nabla \cdot ((\mu + \mu_T \sigma_k^*) \nabla k) + P_k - \beta_0^* \rho \omega k \quad (6)$$

For solving the specific turbulence dissipation rate ω , the following equation is used:

$$\rho(\mathbf{u} \cdot \nabla)\omega = \nabla \cdot ((\mu + \mu_T \sigma_\omega) \nabla \omega) + \alpha \frac{\omega}{k} P_k - \rho \beta_0 \omega^2 \quad (7)$$

with the kinematic eddy viscosity

$$\mu_T = \rho \frac{k}{\omega}$$

and again the production term

$$P_k = \mu_T (\nabla\mathbf{u} : (\nabla\mathbf{u} + (\nabla\mathbf{u})^T)).$$

The k - ω model constants are predefined with the following values [2]:

$$\alpha = \frac{13}{25}; \quad \sigma_k^* = 0.5; \quad \sigma_\omega = 0.5; \\ \beta_0 = \frac{9}{125}; \quad \beta_0^* = 0.09$$

In both simulation tools these predefined model constants are used unmodified in all studies.

3.3 Model Input

The constant density $\rho = 1.18415 \frac{kg}{m^3}$ and the dynamic viscosity $\mu = 1.85508 \cdot 10^{-5} Pa s$ are defined as the material properties for the fluid. The boundary condition ‘‘Velocity Inlet’’ is chosen at $z = -2 m$, i.e. the normal inflow velocity is defined with a constant value. The ‘‘Pressure Outlet’’ boundary condition is located opposite to the inlet at $z = 2.4 m$. Here, the relative pressure is set to $p = 0 Pa$, which means the prevalent pressure equals the atmospheric

pressure. For the walls a “No-slip” condition is defined.

As initial conditions for the flow region, the relative pressure is set to $p_0 = 0 \text{ Pa}$, the turbulent kinetic energy to $k_0 = 0.001 \frac{\text{m}^2}{\text{s}^2}$, and the turbulent dissipation rate to $\varepsilon_0 = 0.001 \frac{\text{m}^2}{\text{s}^3}$ and accordingly the specific dissipation rate to $\omega_0 = 1 \frac{1}{\text{s}}$. In addition, the initial velocity is set according to the constant inlet velocity.

A parametric sweep for the inlet velocity in the range from $0.1 \frac{\text{m}}{\text{s}}$ up to $7.2 \frac{\text{m}}{\text{s}}$ by steps of $0.1 \frac{\text{m}}{\text{s}}$ is performed. This range of fluid velocities corresponds to Reynolds numbers from 638 to 45960. The transition from laminar to turbulent flow in a pipe occurs at Reynolds numbers about 2300. In our Venturi tube test set-up this transition is met for velocity values between $0.3 \frac{\text{m}}{\text{s}}$ and $0.4 \frac{\text{m}}{\text{s}}$.

4. Results

4.1 Experimental Results

The pressure distribution in the Venturi tube is a characteristic function of the average flow velocity respectively the volume flow rate. It would be straight forward to validate the CFD models by comparison between the calculated and the measured pressure-velocity characteristic.

Since the average flow velocity is not known in the present set-up, this approach can not be applied. As an alternative, we determine the differential pressure Δp_7 (between p-7 and p-4, cf. Fig. 3) as a function of the differential pressure Δp_1 (between p-4 and p-1, cf. Fig. 3) experimentally as well as numerically in order to validate our CFD models.

In figure 7 the relation between the differential pressures at the outlet Δp_7 and at the inlet Δp_1 for various velocities is shown. For each adjusted air flow velocity at the inlet 60 measurements are performed. For each series of measurements an error indicator is obtained by calculating the standard deviation. The data shows an increasing variation for higher velocities. The obvious interpretation is that the flow is not stationary and/or does not show axis symmetrical behaviour any longer for very high Reynolds numbers.

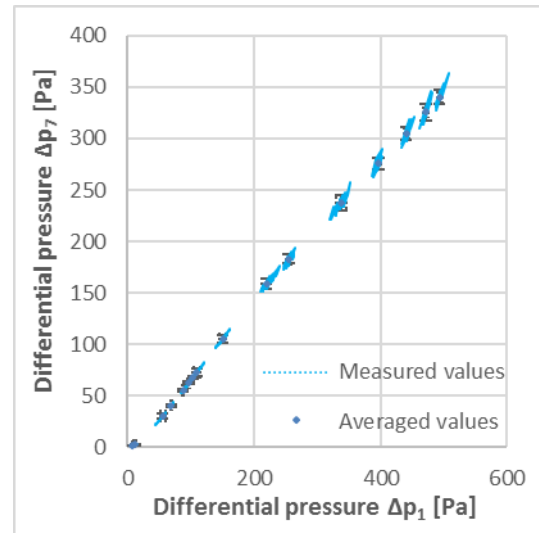


Figure 7. Relation between the differential pressures at the inlet and outlet of the Venturi tube. The blue points represent the measured values for various flow velocities.

4.2 Simulation Results

Numerous simulations using the $k-\varepsilon$ as well as the $k-\omega$ turbulence model were performed in COMSOL Multiphysics® (Version 5.2a) and STAR-CCM+® (Version 12.04.010). All results differ on the one hand, but on the other hand the distribution of the dependent variables (velocity, pressure, turbulent kinetic energy, etc.) look quite similar.

In this section different COMSOL plots for the $k-\varepsilon$ turbulence model for a mean velocity of $6 \frac{\text{m}}{\text{s}}$ are shown exemplary.

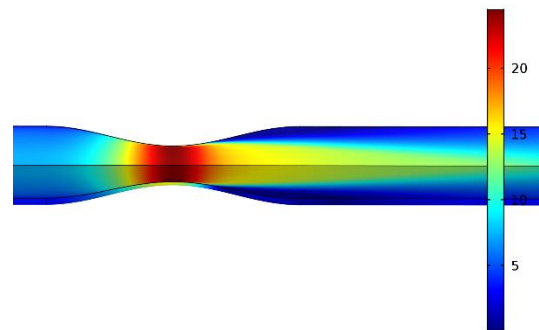


Figure 8. Velocity distribution in the Venturi tube (Unit: $\frac{\text{m}}{\text{s}}$)

Figure 8 shows the velocity distribution. This 3D plot expresses the intensity of the velocity in the

horizontal Venturi tube. The flow enters from the left with an even distribution of the velocity intensity. At the constriction, the velocity of the fluid is tripled, so that the flow separates after it passes the constriction.

The following plots are displayed in the r - z -plane, so that the fluid flows in positive z -direction from bottom to top. Figure 9 is a streamline plot of the velocity in a region behind the constriction.

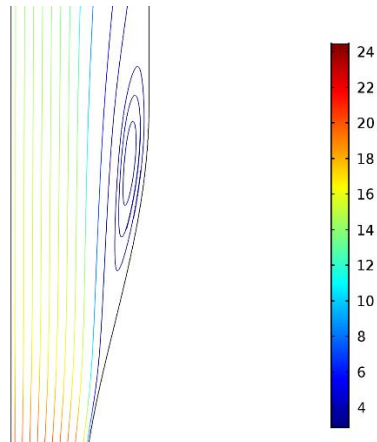


Figure 9. Streamlines behind the constriction (Unit: $\frac{m}{s}$)

Figure 10 presents the pressure distribution in the Venturi tube. Upstream of the constriction the relative pressure is higher than in the middle of it. The reason for this is the increasing velocity to the middle of the constriction (cf. Fig. 8). Behind the constriction, the pressure rises continuously to atmospheric pressure.

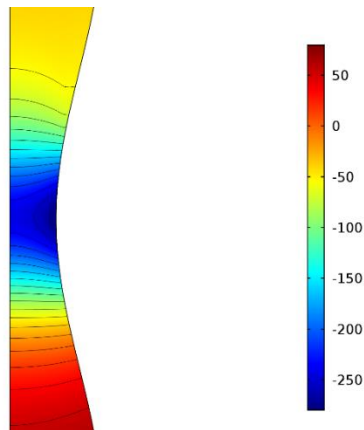


Figure 10. Pressure distribution in the Venturi tube (Unit: $[Pa]$)

In figure 11 the distribution of the turbulent kinetic energy is shown, which describes the dimension of the turbulent fluctuations in a turbulent flow. As expected, the maximum of the turbulent kinetic energy is behind the constriction.

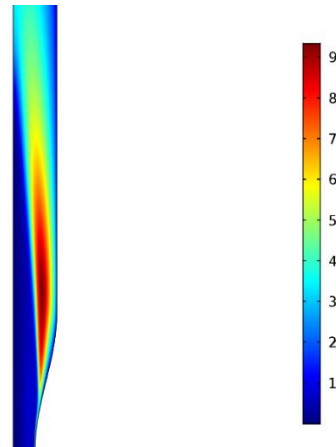


Figure 11. Turbulent kinetic energy distribution behind the constriction (Unit: $\frac{J}{kg}$)

4.2.1 Comparison Between the k - ϵ Turbulence Models and the Measured Data

Figure 12 shows the averaged values from the measured differential pressures and the simulation results from COMSOL Multiphysics® and STAR-CCM+® using the standard k - ϵ turbulence model.

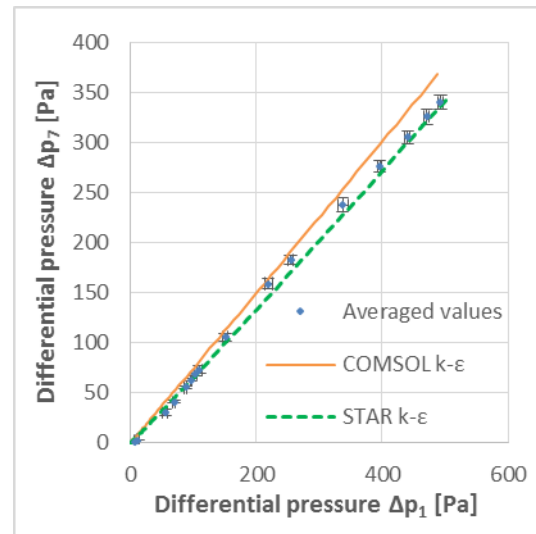


Figure 12. Comparison between the simulation results with COMSOL Multiphysics® and STAR-CCM+® and the measured values.

The numerical results from both simulation tools are close to the measured values, especially for differential pressures $\Delta p_1 < 150 \text{ Pa}$. In general, the slope of the curve representing the COMSOL results is more steep than the one for the STAR results. In addition, the COMSOL results deviate more from the measured values for higher differential pressures Δp_1 .

4.2.2 Comparison Between the $k-\omega$ Turbulence Models and the Measured Data

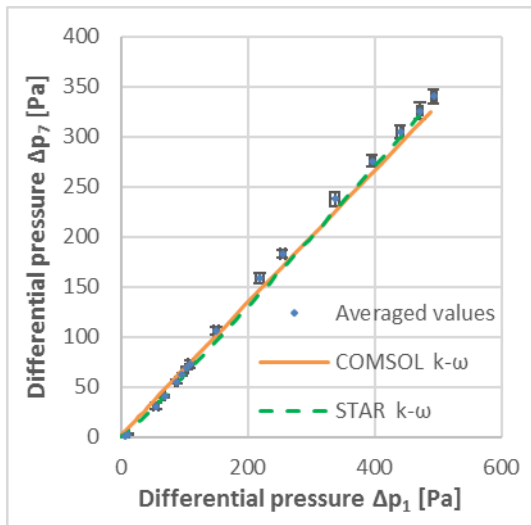


Figure 13. Comparison between the simulation results with COMSOL Multiphysics® and STAR-CCM+® and the measured values.

Using the $k-\omega$ turbulence model the simulation results from COMSOL Multiphysics® as well as STAR-CCM+® are in good agreement with the measured data for a larger range of the differential pressures in contrast to the $k-\varepsilon$ turbulence model results. Both curves (cf. Fig. 13) lie slightly above the experimentally measured values for $\Delta p_1 < 150 \text{ Pa}$ and slightly below the values for $\Delta p_1 > 150 \text{ Pa}$.

4.3 Characteristic Curve for the Venturi Tube

In this case, the $k-\omega$ turbulence model results are superior to those obtained from the $k-\varepsilon$ turbulence model. Thus, the $k-\omega$ results are used to determine the characteristic curve for the Venturi tube used in the experimental test set-up.

The characteristic curve, which indicates the average flow velocity as a function of the differential pressure Δp_1 , is shown in Figure 14.

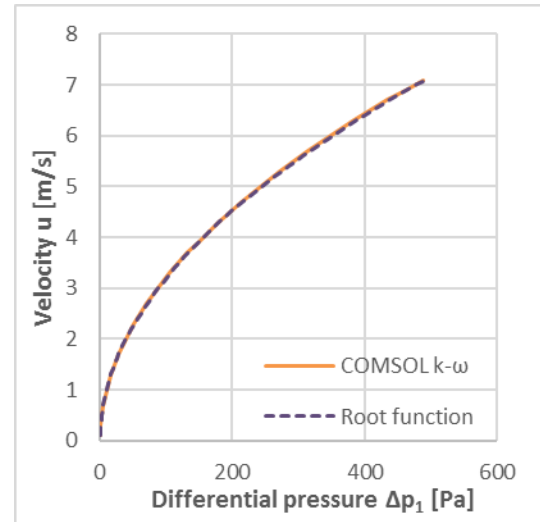


Figure 14. Characteristic curve for the Venturi tube

This curve can be fitted by the following root function quite well (cf. Fig. 14):

$$u = 0.32 \frac{m}{s} \sqrt{\Delta p_1 \frac{1}{Pa}} \quad (8)$$

Figure 15 presents the characteristic curves which are obtained from the results from COMSOL Multiphysics®, STAR-CCM+® and by using Bernoulli's equation.

Again, the curves from the simulations tools are very close to each other, while the velocity values, which are obtained from Bernoulli's equation, are higher, especially at higher differential pressures, as expected. In contrast to the laminar state the turbulence increases the drag in the flow. Therefore, a higher pressure gradient is needed to reach a certain velocity.

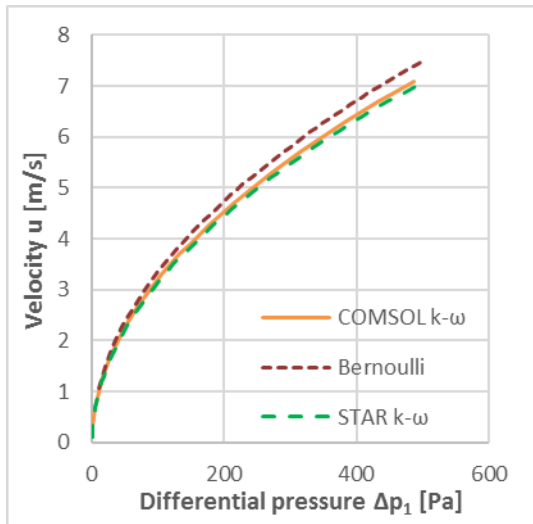


Figure 15. Characteristic curves from COMSOL Multiphysics®, STAR-CCM+® and Bernoulli's equation

5. Conclusion

As a conclusion, both commercial CFD tools, i.e. COMSOL Multiphysics® and STAR CCM+®, are suitable for the simulation of the flow in the Venturi tube. The simulation results are in good agreement with experimentally determined measured data. In the case under consideration the $k-\omega$ turbulence model results are closer to the measured data for a larger range of the differential pressures in comparison to the $k-\varepsilon$ model results. Nevertheless, both turbulence models show deviations for very high Reynolds numbers. From the variations in the experimental measurements for high velocities can be concluded that the assumptions of 2D axis symmetric and stationary flow are not fulfilled in those cases.

Furthermore, we have shown, that the characteristic curve for the Venturi tube can be determined by simulation instead of time consuming and expensive measurements.

The necessity for full 3D and/or unsteady modelling or alternative turbulence models will be topic of further projects.

6. References

1. Jürgen Eichler, *Physik für das Ingenieurstudium*, S.76-77, Springer Vieweg, Wiesbaden, 2014
2. D.C. Wilcox, *Turbulence Modeling for CFD*, 2nd ed., DCW Industries, 1998.
3. COMSOL AB, *CFD Module User's Guide*, Version 5.2a, 2016.